International Journal of Ecological Science and Environmental Engineering
2015; 2(3): 17-29
Published online July 30, 2015 (http://www.aascit.org/journal/ijesee)
ISSN: 2375-3854

AASCIT American Association for Science and Technology

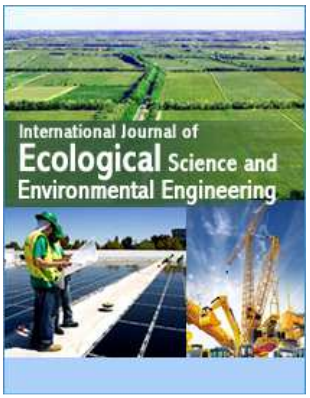

Keywords
Adsorption,
Cationic Dyes,
Sugarcane Bagasse,
Surface Acidity/Basicity,
Point Zero Charge

Received: July 12, 2015
Revised: July 22, 2015
Accepted: July 23, 2015

Adsorption of Safranin O from Aqueous Phase Using Sugarcane Bagasse

M. Farahani, M. Kashisaz, S. R. S. Abdullah*

Department of Chemical & Process Engineering, Faculty of Engineering and Built Environment, University Kebangsaan Malaysia, UKM Bangi, Malaysia

Email address
rozaimah@eng.ukm.my (S. R. S. Abdullah)

Citation
M. Farahani, M. Kashisaz, S. R. S. Abdullah. Adsorption of Safranin O from Aqueous Phase Using Sugarcane Bagasse. *International Journal of Ecological Science and Environmental Engineering.* Vol. 2, No. 3, 2015, pp. 17-29.

Abstract
Three treatments (untreated, NaOH-treated and H_2SO_4-treated) of sugarcane bagasse (SB) were investigated for their effectiveness as absorbent for removal of safranin O, a cationic dye, from water and characterized by Fourier transform infrared spectroscopy (FTIR) and scanning electron microscopy (SEM). Effects of pH, initial dye concentration and contact time were studied in batch mode; zero point charge and surface chemistry were determined; and isotherm models and kinetic equations were developed. Peak adsorption was achieved at pH 10. The adsorption capacity was enhanced by increasing the initial concentration of safranin O. When acidity and basicity were determined by the Boehm method, more acidic groups were found to dominate on the surface of SB. The dye adsorption experimental data were analyzed using both Freundlich and Langmuir models. The Langmuir model showed a superior fit over that of the Freundlich model for the three adsorbent treatments. Lagergren-first-order and pseudo second-order models were used to determine the adsorption kinetics; the pseudo second-order model proved to be the optimum model. The maximum adsorption volume was found to be 58.853, 62.884 and 54.822 $mg.g^{-1}$ for untreated, NaOH-treated and H_2SO_4-treated SBs, respectively. Adsorption reached equilibrium at approximately 1020 minutes (17 hrs). This study suggests that SB is a good candidate for a low-cost adsorbent.

1. Introduction

Dyes and pigments are an important category of water contamination[1]. Indeed, discharge of these pollutants into water resources can result in reduction of light diffusion and consequently reduction of the photo-synthetic efficiency of aquatic plants. Furthermore, these contaminants heighten the chemical oxygen demand (COD) of the effluents. Finally, dyes are known to be potentially toxic or even mutagenic [2-4].

Safranin O [listed in C.I.as Basic Red 2 (BR2)] is a typical organic dye, a member of the Quinone–Imine category. Safranin O is widely applied for counterstaining targets. For instance, it marks yellow as a metachromatic procedure for cartilage staining [5]. Commercial Safranin O, a cationic dye [6], is a reddish or brownish-red powder and has blood-red solution style in water. A number of physicochemical procedures are available for elimination of dyes from aqueous solutions: membrane filtration [7,8], flocculation [9], chemical oxidation [10,11,12], electroflotation [13], ozonation [14,15], ion-exchange [16], adsorption [7-18] and irradiation [19]. Of these techniques, adsorption has been found to be the most influential method with the advantages of low operational cost, low sludge production and applicability in cases of low contaminant concentrations [20].

Activated carbons, carbon blacks, and activated carbon fibres are among the carbonaceous materials that are famous for their extensive specific surface area, pore volumes, chemical inertness, and mechanical stability [21,22]. They are also widely known to remove dyes [23,24]. However, the adsorption process with activated carbon is expensive [25-27].

Recently, attention has turned to the production of low-cost adsorbents from waste materials [27,28]. Studies have investigated the applications of these inexpensive adsorbents for removal of specific pollutants, mainly dyes and heavy metals, from aqueous phase [29, 30]. The use of some agricultural by-products such as sawdust, bark, tree fern and SB as inexpensive substitutes for more conventional adsorbents is gradually gaining interest in the industry. The constituents of these materials, which include polymers, cellulose, lignin, and hemicelluloses, may be responsible for their natural exchange capacity and general sorptive characteristics [25, 31].

In this study, SB was used as an agent to remove the dye safranin O from aqueous solution [25]. Three treatments of the SB adsorbent were used, namely, untreated, NaOH-treated and H_2SO_4-treated. SB was treated by H_2SO_4 and NaOH to investigate modification effect on adsorption capacity. Fourier transform infrared (FTIR) and (SEM) were used to characterize the SB [31]. The chemical modification of sorbents with acids or bases was conducted to enhance their adsorption capacity and to examine potential application of this new sorbents in basic dye wastewater treatment. The acid and base were used to modify the adsorption capacity of adsorbent in elimination of basic dyes from wastewater [32].

The kinetics of adsorption and equilibrium parameters were determined to explain the outcomes.

2. Materials and Methods

2.1. Materials

SB was collected from a local fresh juice shop in Bangi, Malaysia. The SB was washed with distilled water and then dried in an oven at 80°C degrees for 24 hours [33]. The material was then ground to a fine powder (particle size range is 0.02–2000 μm)[33] in a blender (Panasonic, China). Untreated SB was prepared by washing, drying (at 80°C degrees for 24 hours), and grinding only. The 300 g of ground powder was divided into three equal parts, one of which was untreated while the other parts were soaked in either the acid solution (0.01 N of H_2SO_4, 99.96%) or the base solution (1 N of NaOH, 99.96%) in 1 L for 24 hours at room temperature (29°C). After treatment, both powders were thoroughly rinsed with distilled water and then dried overnight separately in an oven. The weight loss of H_2SO_4, and NaOH treated material was roughly 28% and 43%, respectively.

Cationic dye safranin O was purchased from Sigma–Aldrich (Malaysia) and used without further purification as an adsorbate. The stock solution was prepared by dissolving 1 g dye in 1000 mL distilled water [26]. The chemical structure of safranin O is shown in Fig. 1.

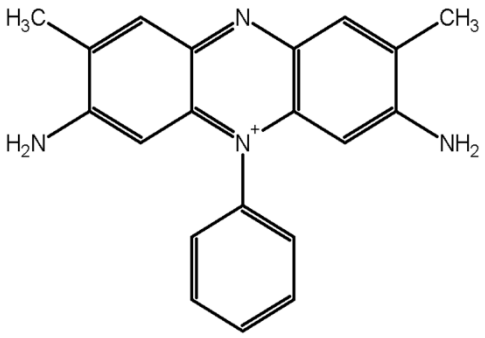

Fig. 1. *The chemical structure of safranin O as a cationic dye.*

2.2. Analytical Method

The concentrations of safranin O in the samples before and after the adsorption process were quantified using UV–visible spectrophotometer (Perkin Elmer Lambda 35, U.S.). The maximum wavelength (λ_{max}) for safranin O absorbance was 516 nm. In addition, the pH of the solutions during the study was determined by pH meter (Cyber Scan 510, U.S.).

2.3. Characterization of the Adsorbent

Fourier transform infrared spectroscopy (FTIR) of SB samples was recorded by Nicolet 6700 Thermo Scientific-FITR spectrometer (USA). The FTIR analysis was performed on the SB and acid and base treated SBs to determine the surface functional groups in range 4000–400 cm^{-1}.

Scanning electron microscopy (SEM) micrographs of samples were obtained using a scanning electron microscope (ZEISS SUPRA 55 VP, Germany). The morphology of untreated, acid treated and base treated SB before and after of adsorption was analyzed at a voltage of 10 KV. All sample surfaces were gold-coated before analysis.

The point zero charge (pH_{pzc}) of SB [34] was determined by solid addition using 0.01 M KNO_3 solution. The process was conducted in 250 mL conical flasks (10 conical flasks) with stopper cork, each containing 90 mL of 0.01 M KNO_3 solution. The initial pH (pH_i) of the solution in the conical flasks was modified in the range of pH 2 to pH 11 at intervals of 1 pH value by adding 0.2 N HNO_3 or 0.2 M KOH. Subsequently, the volume of the solutions was modified to 100 mL by adding KNO_3 solution at the same concentration. Then the initial pH_i of the solutions was precisely measured and set to one of the pH settings. At this stage, 1g of SB adsorbent was added to each conical flask, and the flasks were covered instantly. Subsequently the suspensions were shaken manually and allowed to equilibrate for 48 h with intermittent manual shaking (150rpm). The difference between the initial (pH_i) and final (pH_f) pH values ($\Delta pH = pH_i - pH_f$) was plotted versus the pH_i. The pH_{pzc} is the point of intersection of the obtained graph with x-axis at $\Delta pH = 0$.

The acid–base titration experiments using Boehm titration

[35] were employed to investigate the existence of acidic and basic sites on the SB surface; results are shown in Table S.1. Alkaline solutions (0.1 N of NaOH, 0.1 N of $NaHCO_3$ and 0.1 N of Na_2CO_3) were used to neutralize all acidic sites while 0.1 N of HCl solution was used to neutralize the basic sites. The acidic and basic sites were investigated by adding 50 mL of 0.1 N titrating solutions and 1 g of SB to all 250 mL conical flasks. The flasks were shaken gradually in a constant temperature water (25°C) bath and left for 4 days. Finally, 10 mL of each sample was titrated with 0.1 N of HCl or 0.1 N of NaOH solutions.

2.4. Adsorption Study

The adsorption of safranin O on SB was studied in batch mode. Different parameters, including pH variation, initial dye concentration (5, 10, 15, 20, 25, 30, 35, and 40 mg/L) and contact time (5, 10, 15, 30, 60, 90, 120, 180, 300, 420, 540, 660, 780, 900, 1020, 1140 and 1260 min) were assessed. The initial pH of the safranin O solutions was adjusted by adding 0.5 N of HCl or 0.5 N of NaOH solutions. The adsorbate solutions (250 mL) with different initial safranin O concentrations (from 5 to 40 gm/L at 5 mg/L intervals) were placed in 250 mL conical flasks. One g of adsorbent (4 gL-1)was then added as an optimum dosage to each flask and equilibrated in a shaker at 200 rpm under ambient temperature conditions. All isotherm experiments were conducted in 250 mL conical flasks. Adsorbate solutions (250 mL) of desired initial concentrations (5–40 mg/L at 5 mg/L intervals) were equilibrated in a shaker at 200 rpm using 1 g of adsorbent under ambient temperature conditions. The adsorption capacity values at equilibrium (qe) were calculated using the following equation:

$$q_e(mg/g) = (C_0 - C_e) \times \frac{V}{W} \quad (1)$$

where C_0 is the initial adsorbate concentration (mg/L), C_e is the adsorbate concentration at equilibrium (mg/L), V is volume of the solution (L) and W is mass of the adsorbent (g).

The kinetics studies were conducted to measure the time-dependent uptake of safranin O onto SB. The studies were carried out using 250 mL conical flasks containing 250 mL of adsorbate solutions with the various initial safranin O concentrations (between 5 and 40 mg/L at 5 mg/L intervals). To each flask, 1 g of adsorbent was added. Subsequently, it was equilibrated in a shaker at 200 rpm under ambient temperature conditions and at predetermined time intervals (5, 10, 15, 30, 60, 90, 120, 180, 300, 420, 540, 660, 780, 900, 1020, 1140 and 1260 min). The adsorbate solution of the specified flask was then filtered and analyzed for its dye concentration.

3. Results and Discussion

3.1. Characterization of Adsorbents

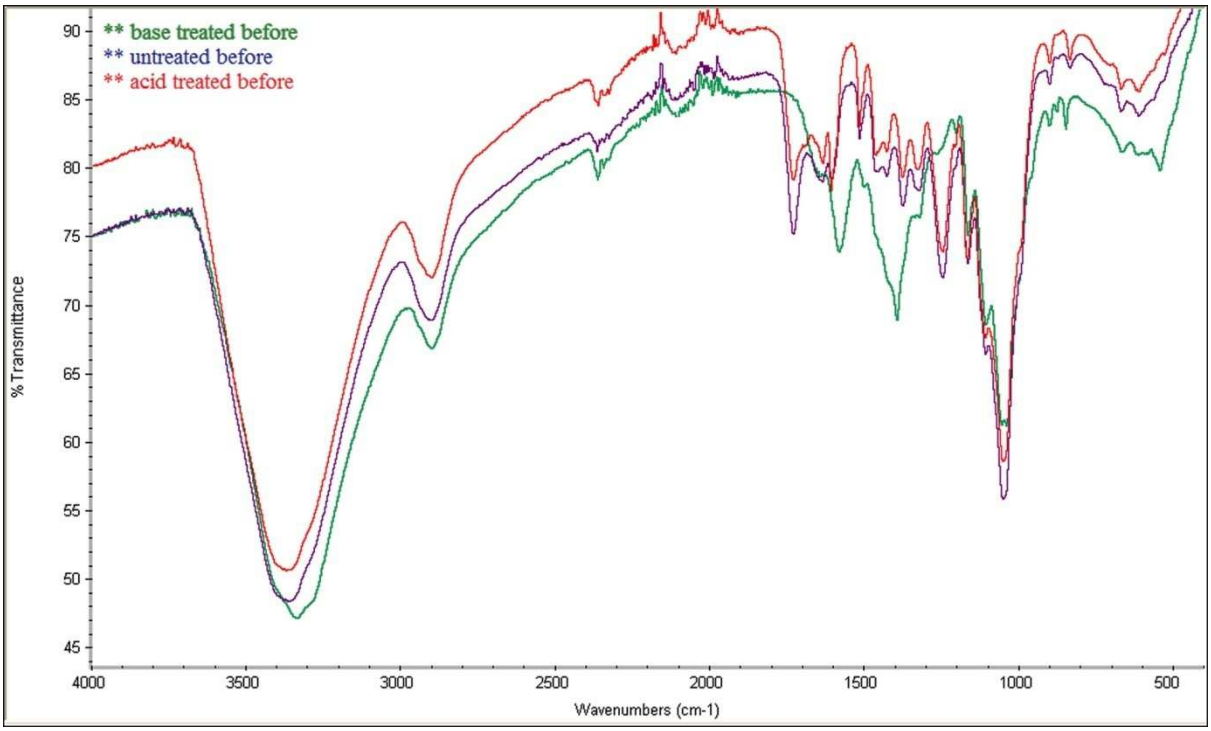

Fig. 2. *FTIR spectra of untreated SB, acid treated SB and base treated SB before adsorption.*

The FTIR spectrum of samples indicated weak and broad peaks in the region of 3840 - 600 cm^{-1} as shown in Fig. 2. The FTIR band could reveal that carboxyls, lactones, and phenols groups as reported by surface analysis with Boehm method. The treated and untreated SBs displayed the strong peak of hydroxyl (O–H) group at wave number 3350 cm^{-1}. The CH_3 (alkane group) corresponded closely to the 2920 cm^{-1} band. The carboxyl groups equivalent to carboxylic groups and

C-OH vibrations in the range of 1200 to 1300 cm^{-1} and a carbonyl (C=O) at 1734 cm^{-1} stretching vibrations in ketones, aldehydes, lactones. The band of alkenyl C=C stretch was revealed at 1640 cm^{-1}. The band 1427 cm^{-1} might be as a result of amides functional groups of primary amides and aliphatic amides [36]. The vibration of band 600 cm^{-1} was caused by aromatic C-H bending. There was no significant difference between untreated and treated SBs, thus the acid and base treatment had no obvious impact on the principal chemical structures of SB.

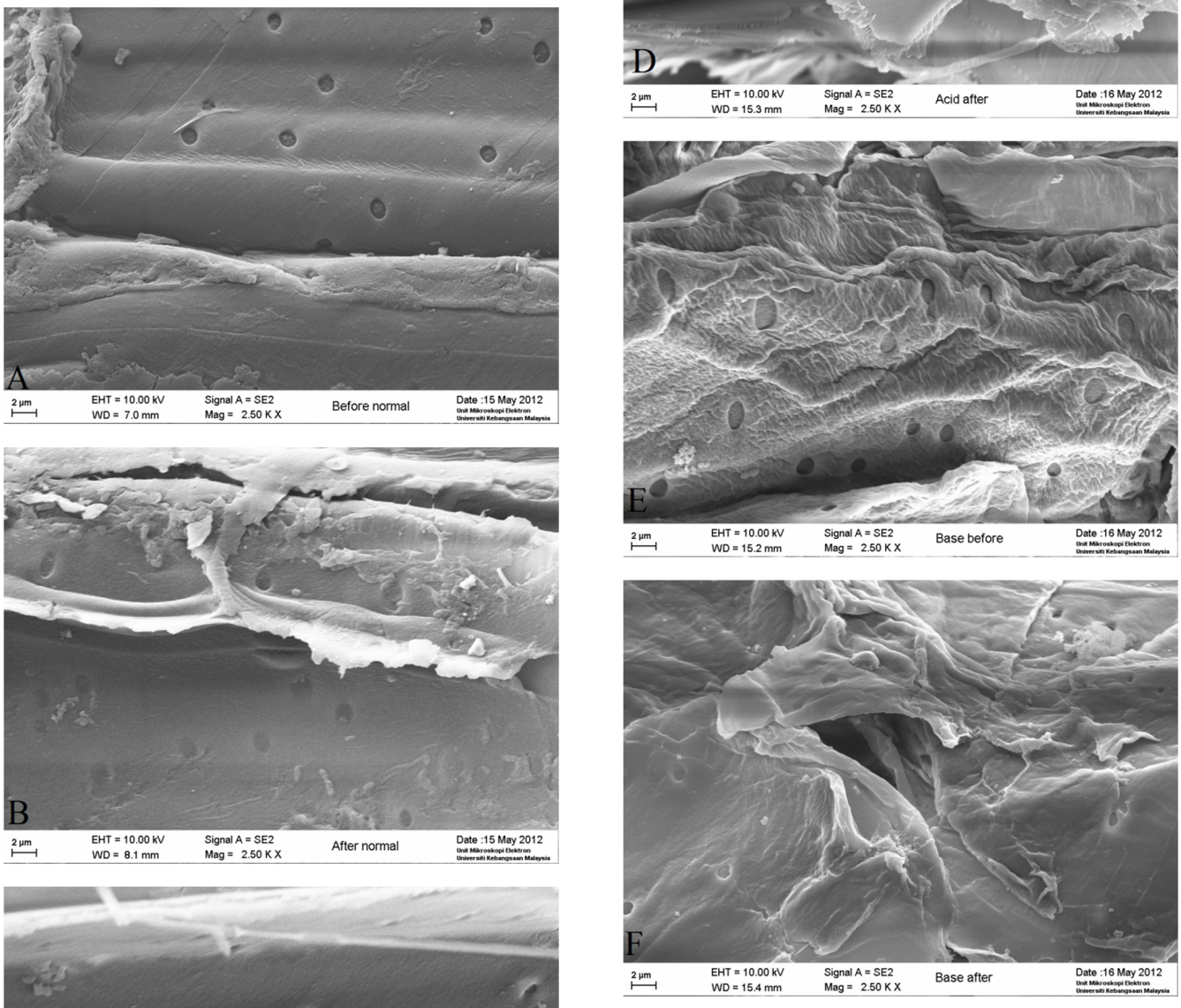

Fig. 3. *SEM image of (A and B) untreated SB, (C and D) acid treated SB and (E and F) base treated SB.(A,C and E)show before while (B,E and F) demonstrate after dye adsorption process.*

The SEM image (Fig. 3A) of untreated SB at 7 mm magnification shows irregular expanded porous surface before the adsorption process. The magnified image of untreated SB (Fig. 3B) shows well coverage of empty pores. Figs. 3C-F shows the images of acid treated and base treated SB before and after adsorption. Based on Fig 3, it is obvious that all samples were irregularly shaped (2 µm). The changes in

external morphology after acid and base treated can be investigated by comparing with Figs 3 before the adsorption. It can be observed that the surface of base treated (Fig. 3E) was much cruder than untreated SB and acid treated (Fig. 3A and C), which can be attributed to this fact that lignin and hemicelluloses dissolved or degraded in the basification procedure [37]. The surface of base treated SB (Fig. 3F) became much smoother after adsorption of safranin O when compared to before adsorption (Figs. 3E and 3F). The porous surface of all samples was almost well occupied with safranin O after adsorption process.

3.2. Effect of Initial pH

One of the potentially most crucial parameters in adsorption process in aqueous solution is the effect of pH [38]. The effect of pH on the amount of dye adsorbed was studied by varying the initial pH under constant process parameters at equilibrium conditions. The effect of pH was studied for the three adsorbent treatments, as shown in Fig. 4.

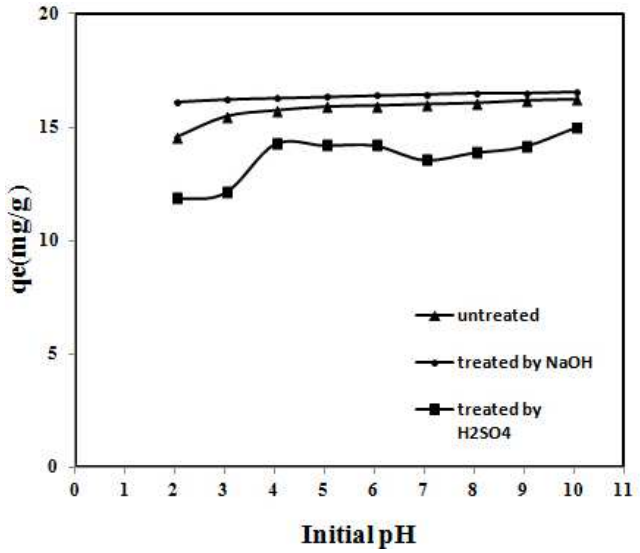

Fig. 4. *The effect of pH on the adsorption of safranin O on untreated, NaOH-treated and H_2SO_4-treated samples. Conditions: Initial concentration 40 mg/L, mass of adsorbents 1gr, temperature 25°C, time 24 hr.*

The figure shows that the NaOH-treated indicated no more difference of dye adsorption in pH range 2 to 10. Therefore, any advantage of the NaOH pretreatment of SB is independent of the solution pH, probably due to the negative charge of the surface adsorbent (OH^-) and the positive charge of safranin O solution. However, the adsorption capacity is 16.55 mg/g for NaOH-treated bagasse (Fig. 4).

According to Fig. 4, for the H_2SO_4-treated SB the highest extent of adsorption (14.95 mg/g) took place at pH 10 (there is no pH_{pzc} for the H_2SO_4-treated sample as in Fig. 4). At lower pH values between 2 and 5, the quantity of the adsorbed dye shows the lowest value.

For the untreated sample, it was evidence that the adsorbent showed better adsorption capacity in the pH range from 5 to 10 as seen in Fig. 4 (pH_{pzc}= 6.6 from Fig.5). The reason for this might be the higher adsorption ability of the dye molecules by the adsorbent surface which are negatively charged. pH 10 indicating a strong basic medium was found to be the most favorable as the maximum removal of dye was observed at this pH condition (maximum adsorption of 16.23 mg/g). Since one of the basic substance in SB is cellulose, thus at the place where water comes in contact with the outermost part of the cellulose, a negatively charged medium is established [39]. Due to the fact that safranin O is a cationic dye, it thus exhibits attractive tendencies whenever it is within the vicinity of structures with anionic effect, of which most adsorbents are good examples.

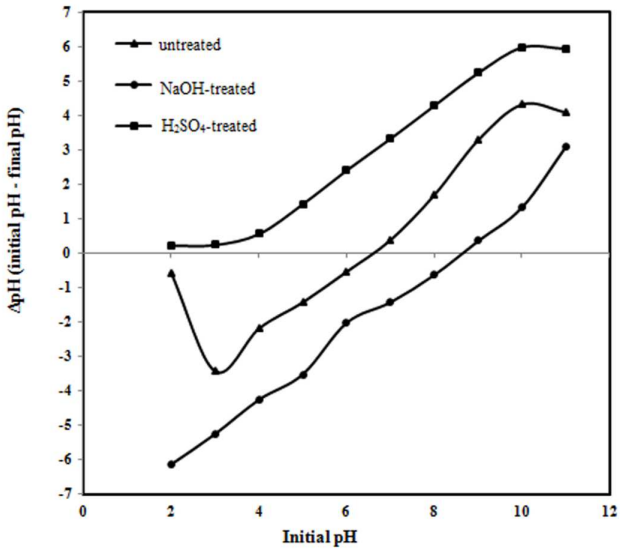

Fig. 5. *Point of zero charge (pH_{pzc}) plot for untreated, NaOH-treated and H_2SO_4-treated SB using 0.01 M of KNO_3.*

3.3. Effect of Initial Concentration and Contact Time

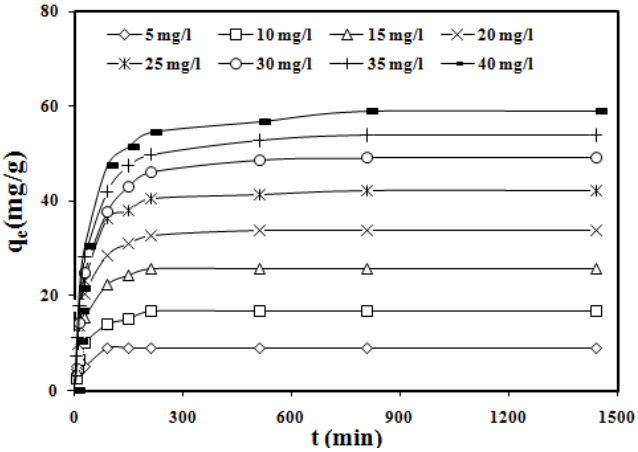

Fig. 6. *concentration effect of adsorption of Safranin O by untreated SB (pH=10).*

The effect of initial dye concentration and contact time on the removal of safranin O using each SB treatment is shown in Figs. 6-8. The removal of dye increased with increasing dye concentration. The adsorption increased with an increase in contact time. The dye removal is rapid at the initial stages

of adsorption at different initial concentrations. By increasing contact time, the adsorption gradually decreased until reaching equilibrium. The solution pH was kept at 10.

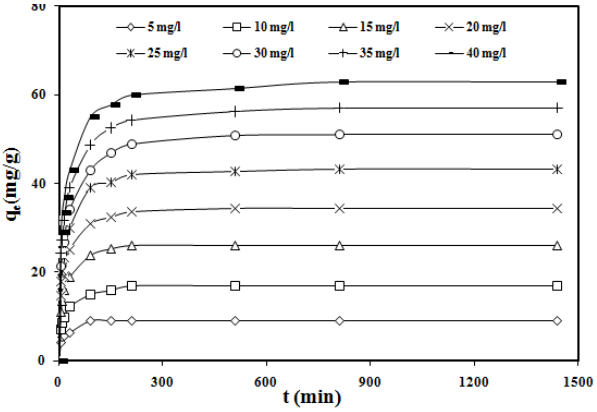

Fig. 7. *concentration effect on adsorption of Safranin O by NaOH-treated SB(pH=10).*

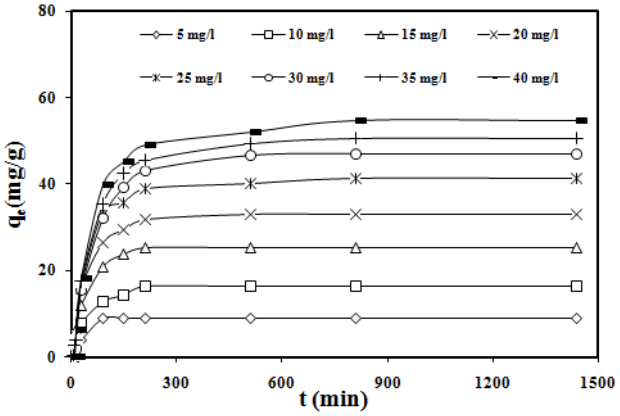

Fig. 8. *concentration effect on adsorption of safranin O by H_2SO_4-treated SB(pH=10).*

At lower concentrations, equilibrium was attained at around 11 hrs (660 mins) (Figs. 6-8), but higher initial concentrations required a longer time to reach equilibrium, the maximum equilibrium time was around 1020 mins (17 hours) (Figs. 6-8). The adsorption capacities (q_e) for the uptake of safranin O versus contact time in the maximum initial concentrations for untreated, base-treated and acid-treated SB were 58.853, 62.884 and 54.822 mg/g, respectively. All the experiments were conducted under the same conditions.

The adsorption process can be divided into two sections. In the first section adsorption is high at the initial stages (0 to 90 min) due to rapid attachment of safranin O to the surface of the SB. Thereafter during the second section adsorption took place at a slower rate until equilibrium was achieved.

3.4. Adsorption Isotherm

In order to evaluate safranin O adsorption onto untreated, NaOH-treated, and H_2SO_4-treated SB, the Langmuir and Freundlich isotherm models were used [1,3,4,8,12,13,17,18, 24,26-32,40,41]. The Langmuir model hypothesizes that adsorption occurs onto a monolayer surface of adsorbent. This model posits no attraction between adsorbed molecules [42]. The Langmuir model and its linearized form are illustrated by the following two equations:

$$q_{e=}\frac{q_m k_L c_e}{1+k_L c_e} \tag{2}$$

$$\frac{C_e}{q_e}=\frac{1}{q_m k_L}+\frac{C_e}{q_m} \tag{3}$$

where q_e represents equilibrium adsorption capacity; $q_m$is the maximum adsorption capacity required to produce a complete monolayer on the surface (mg/g); and k_L is the Langmuir constant related to the energy of adsorption (L/mg). The values of q_m and k_L can be derived from the slope and intercept of the plot C_e/q_e versus C_e.

The Freundlich model, on the other hand, describes the phenomenon of adsorption empirically on heterogeneous surfaces in a multilayer adsorption system [43]. The Freundlich model and its linearized form are illustrated by the following equations:

$$q_{e=}k_F C_e^{1/n} \tag{4}$$

$$\log(q_e)=\log(k_F)+\frac{1}{n}\log(C_e) \tag{5}$$

In these equations, n and k_F are Freundlich isotherm constants related to the adsorption intensity and adsorption capacity of the adsorbent (mg/g), respectively. These constants can be obtained from the slope and intercept of the plot of logC_e against logq_e [44].

The equilibrium data were modeled using the Freundich and Langmuir models. The experimental data of equilibrium adsorption was compared to the isotherm models, as shown in Fig. 9. The isotherm was found to be linear over the entire concentration range studied with a good linear correlation coefficient (R^2). The highest value of the linear correlation coefficient was used to determine the best fitting model with the experimental data. The parameters tested by the two models for the three types of SB adsorbents are listed in Table 1. In Fig.9, the Langmuir model showed a better fit with the isotherm data with its higher R^2 value than did the Freundich model, indicating the removal of safranin O was monolayer adsorption by the untreated sample. Moreover, Fig.9 showed that both Langmuir and Freundlich models gave good fit with the isotherm data, indicating the base treatment followed by adsorption on monolayer and multilayer, and the acid treatment demonstrated a better fit with the Langmuir model than with the Freundlich model due to the higher R^2 values (Table 1). Furthermore, these outcomes were evident by non-linear plots (Fig. 9). The values of exponent n are in the range of acceptable adsorption ($1<n<10$) (Table 1) [38].

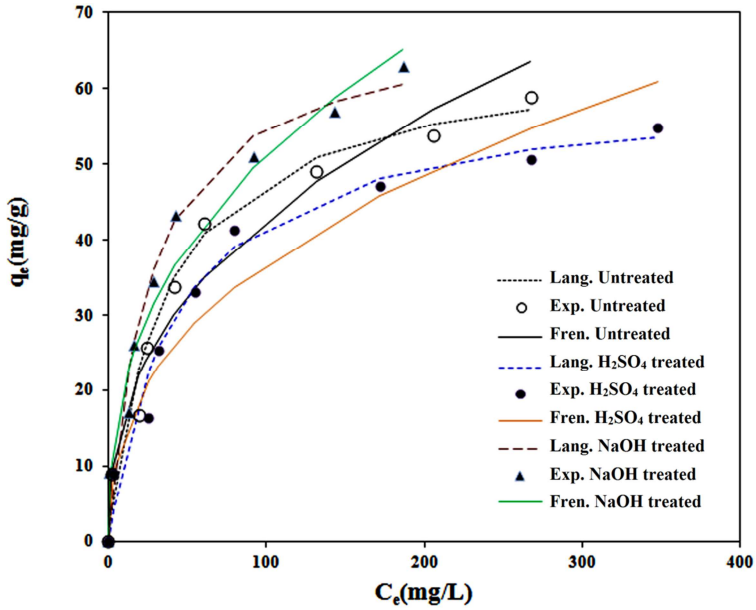

Fig. 9. *Comparison of adsorption capacity with two isotherm plots for untreated, NaOH-treated, H_2SO_4-treated SB.*

Table 1. *Isotherm parameters for Safranin O adsorption by untreated, acid and base-treated SB.*

Adsorbents	Langmuir constants			Freundlich constants		
	K_L(L/g)	a_L	R^2	K_F(mg/g)(L/mg)$^{1/n}$	n	R^2
Untreated	1.8021	0.0278	0.9839	6.6373	2.4728	0.9530
NaOH treated	2.6455	0.0384	0.9790	8.5986	2.5833	0.9554
H_2SO_4 treated	1.3966	0.0232	0.9872	5.7408	2.4783	0.9450

3.5. Adsorption Kinetics

Lagergren first-order [45] and pseudo-second-order [1-3,8,12,13,15,17,24,26-32,33,37,38,40,41,43,44,45-49] kinetics models were utilized to determine the specific rate constants of adsorption of afranin O in the three adsobent system. The kinetics study for the adsorption of Safranin O on untreated, acid-treated and base-treated SB was conducted using varying initial safranin O concentrations. The Lagergren first-order model is shown in the following equation:

$$log(q_e - q_t) = log\, q_e - \frac{k_1}{2.303}t \quad (6)$$

Where q_e and q_t are the adsorption capacities at equilibrium and time t and k_1 is the adsorption rate constant. The values of adsorption capacity and rate constant were calculated from the slope and intercept of the plot of log $(q_e - q_t)$ against t.

The pseudo-second-order reaction in linear form is given as:

$$\frac{t}{q_t} = \frac{1}{k_2 q_e^{\,2}} + \frac{1}{q_e}t \quad (7)$$

where k_2 is the pseudo-second-order rate constant. The values of adsorption capacity and rate constant were derived by the intercept and slope of the plot t/q_t against t.

Two values k_1 and $q_{cal,e1}$ (the amount of adsorption for first order equation) were determined by the slope and intercept of the log$(q_e - q_t)$ plotted against t. Using second order kinetics, k_2 and $q_{cal,e2}$ (amount of adsorption for second-order equation) were obtained from the intercept and slope of t/q_t plotted versus t. The comparison between the results obtained by the two models is presented in Tables 2-4.

Table 2. *Kinetics parameters for the adsorption of safranin O at various initial concentrations on untreated SB.*

		Lagergren first-order			Pseudo-second-order		
C_o (mg/L)	q_{exp} (mg g^{-1})	R^2	k_1 (min^{-1})	$q_{cal,e1}$ (mg g^{-1})	R^2	k_2 (g.mg^{-1} min^{-1})	$q_{cal,e2}$ (mg g^{-1})
5	9.062	0.9661	0.0357	6.899	0.9996	0.0110	9.158
10	16.726	0.8267	0.0233	11.092	0.9996	0.0034	17.007
15	25.732	0.8957	0.0313	17.446	0.9996	0.0026	26.110
20	33.773	0.8378	0.0258	22.709	0.9996	0.0017	34.364
25	42.297	0.8639	0.0196	26.903	0.9995	0.0011	43.103
30	49.059	0.9163	0.0175	34.072	0.9994	0.0008	50.251
35	53.808	0.9460	0.0166	35.958	0.9995	0.0007	54.945
40	58.853	0.9174	0.0143	37.506	0.9997	0.0008	59.880

Table 3. *Kinetics parameters for the adsorption of safranin O at various initial concentrations on NaOH-treated SB.*

		Lagergren first-order			Second-order Kinetics		
C_o	q_{exp}	R^2	k_1	$q_{cal,e2}$	R^2	k_2	$q_{cal,e2}$
(mg/L)	(mg g^{-1})		(min^{-1})	(mg g^{-1})		(g.mg^{-1} min^{-1})	(mg g^{-1})
5	9.118	0.9661	0.0357	4.829	0.9999	0.0232	9.158
10	17.039	0.8267	0.0233	7.764	0.9999	0.0076	17.007
15	26.118	0.8957	0.0313	12.212	0.9999	0.0058	26.316
20	34.424	0.8378	0.0258	15.896	0.9999	0.0036	34.722
25	43.237	0.8639	0.0196	18.832	0.9999	0.0025	43.478
30	51.059	0.9163	0.0175	23.851	0.9999	0.0018	51.546
35	56.916	0.8818	0.0164	25.009	0.9999	0.0174	57.471
40	62.884	0.9174	0.0143	24.672	0.9999	0.0158	63.291

Table 4. *Kinetics parameters for the adsorption of safranin O at various initial concentrations on H_2SO_4-treated SB.*

		Lagergren first-order			Pseudo-second-order		
C_o	q_{exp}	R^2	k_1	$q_{cal,e1}$	R^2	k_2	$q_{cal,e2}$
(mg/L)	(mg g^{-1})		(min^{-1})	(mg g^{-1})		(g.mg^{-1} min^{-1})	(mg g^{-1})
5	9.006	0.9383	0.0267	8.069	0.9986	0.0053	9.200
10	16.412	0.8312	0.0228	13.948	0.9818	0.0008	17.544
15	25.346	0.8986	0.0309	21.938	0.9946	0.0009	26.455
20	33.122	0.8400	0.0253	28.668	0.9670	0.0003	35.971
25	41.356	0.8714	0.0189	32.900	0.9908	0.0003	44.248
30	47.060	0.9242	0.0168	41.908	0.9236	0.0002	49.358
35	50.700	0.9157	0.0115	44.005	0.9835	0.0002	55.556
40	54.822	0.9224	0.0140	44.432	0.9969	0.0003	57.803

The best fit of the models for (untreated, NaOH-treated and H_2SO_4-treated SB) were selected using the highest value of linear regression coefficients value (R^2) and reasonable values of the calculated $q_{cal,e1}$ and $q_{cal,e2}$. The regression coefficient values (R^2) of the second-order model are higher than those of the first-order model in all three adsorbent treatments. The calculated $q_{cal,e2}$ also show good agreement with the experimental $q_{\exp,e}$ values within an error of 2.2 to 9.6%. Therefore, these comparisons suggest that the adsorption process did not follow the first-order model but instead obey the second-order model for all adsorbent treatments.

As seen in Figs. S.1-S.6, the curve fitting plots of t/q_t versus t reveal good fit for the entire adsorption period for safranin O while the plots of $\log(q_e - q_t)$ versus t do not fit as well. Due to the assumption behind the second-order model and the good fit of the second-order kinetic for the entire adsorption period, the adsorption is taken to be chemisorption [38]. Different adsorption capacities of SB and its derivation types are listed in Table 5. Bagasse pith had better adsorption capacity for methyl red by 90.2 mg g^{-1}, while in this study, untreated SB capacity was 58.8 mg g^{-1}. Therefore, this value has shown reasonability of this process in comparison with other amount of adsorption in Table 5.

Table 5. *Adsorption capacities and the adsorbate used for adsorption of safranin O onto SB.*

Adsorbent	Adsorbate	Adsorption capacity (mg g^{-1})	Reference
Bagasse pith(raw)	Acid blue 25	17.5	[50]
Acticated carbon bagasse	Acid blue 80	391	[51]
AC-SB	Acid orange 10	5.7	[52]
Bagasse pith (raw)	Acid red 114	20	[50]
Bagasse pith	Acid red 114	22.9	[53]
Bagasse pith raw	Basic blue 69	152	[50]
AC-Bagasse	Basic red 22	942	[54]
Bagasse pith (raw)	Basic Blue 3	37.5	[55]
Bagasse pith (raw)	Reactive orange 16	34.4	[55]
Bagasse pith (raw)	Methyl Red	90.2	[56]
Bagasse pith (raw)	Congo Red	4.4	[57]
Sugarcane dust	Basic violet 10	50.4	[58]
Sugarcane bagasse	Methylene blue	34.2	[59]
Sugarcane bagasse	Methyl red	54.6	[60]
Untreated Bagasse	Basic red 2 (Safranin O)	58.8	Present work
Bagasse treated by NaOH	Basic red 2 (Safranin O)	62.8	Present work
Bagasse treated by H_2SO_4	Basic red 2 (Safranin O)	54.8	Present work

4. Conclusions

SB was shown to be an inexpensive agricultural industrial adsorbent that can be appropriately used to eliminate safranin O in aqueous solution in a batch method. The safranin O elimination in artificial wastewater by acid and base pre-treated SB was investigated in this study. Untreated and sulfuric acid- and hydroxide sodium-treated SB were utilized in safranin O adsorption with different dye concentrations and pH as well as different contact times. The adsorption efficiency of different adsorbents was in the order: q_e base-treated SB, 62.884 mg g^{-1} >q_e untreated SB, 58.853 mg g^{-1} >q_e acid treated, 54.822 mg g^{-1}. The initial pH10 was obtained as the optimum pH for three adsorbents. The isotherm data indicated the best fit to the Langmuir model, giving evidence that the adsorption took the form of monolayer coverage. The kinetics results were fixed on the second-order kinetic model, and adsorption reached equilibrium at approximately 1020 mins (17 hours).

Supporting Information

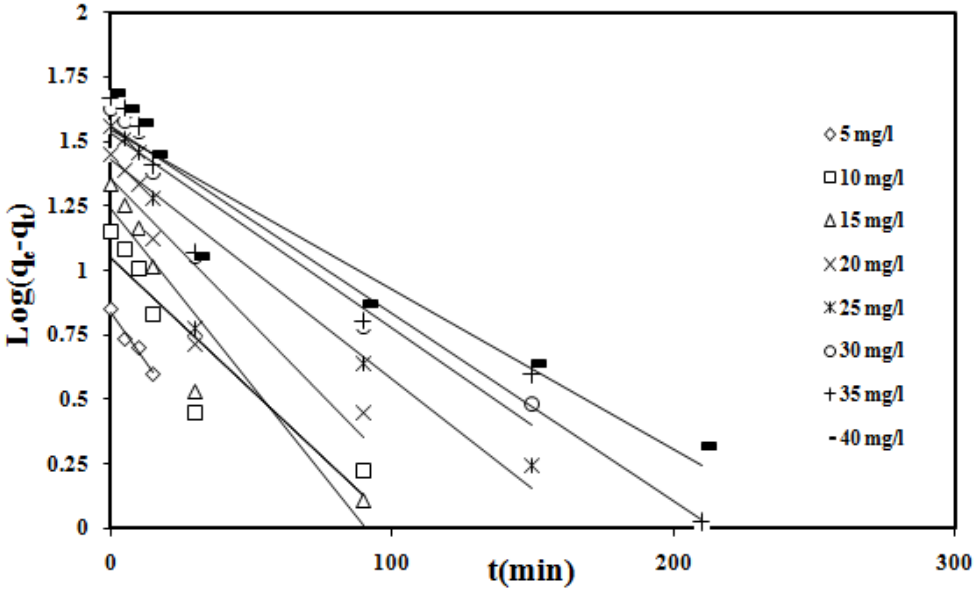

Fig. S.1. *Linear plot of first order model for untreated sample in the entire adsorption period.*

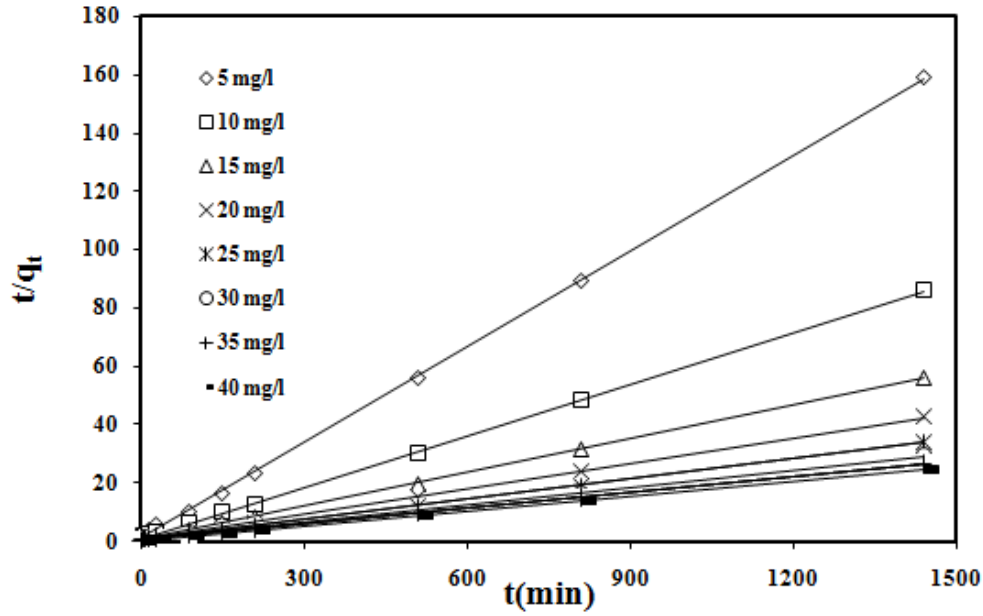

Fig. S.2. *Linear plotting of second order model for untreated sample in the entire adsorption period.*

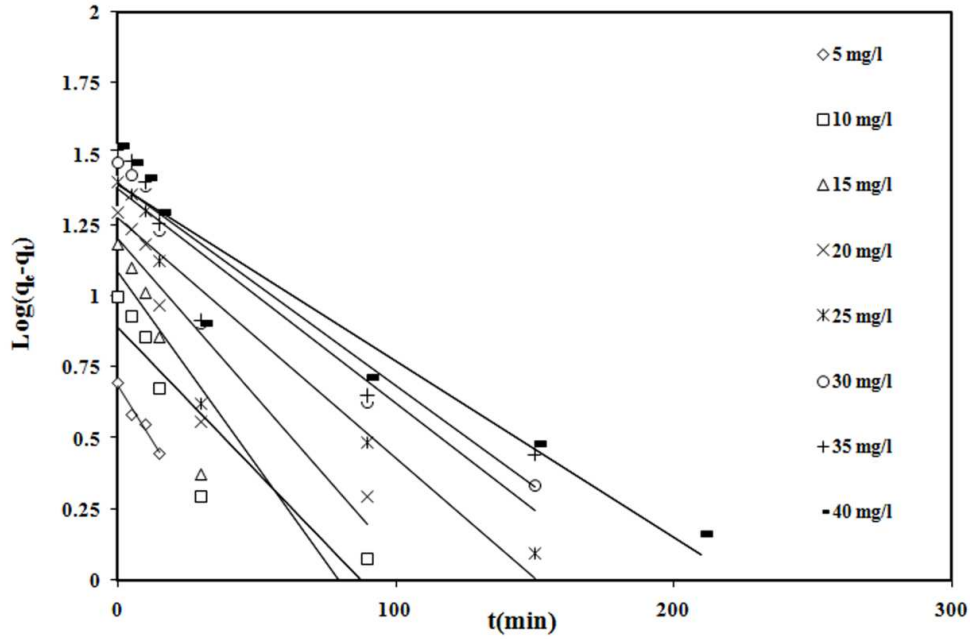

Fig. S.3. *Linear plot of first order model for base-treated sample over the entire adsorption period.*

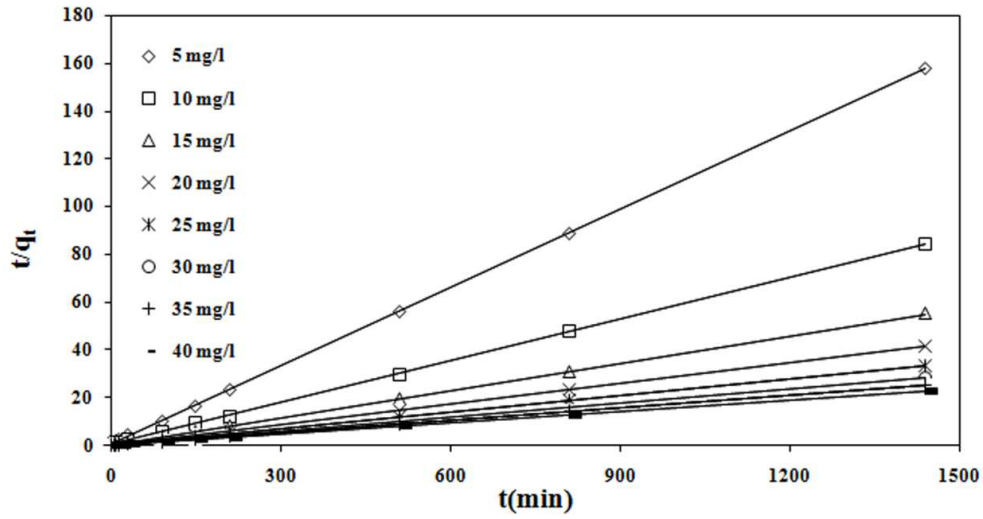

Fig. S.4. *Linear plot of second order model for base-treated sample over the entire adsorption period.*

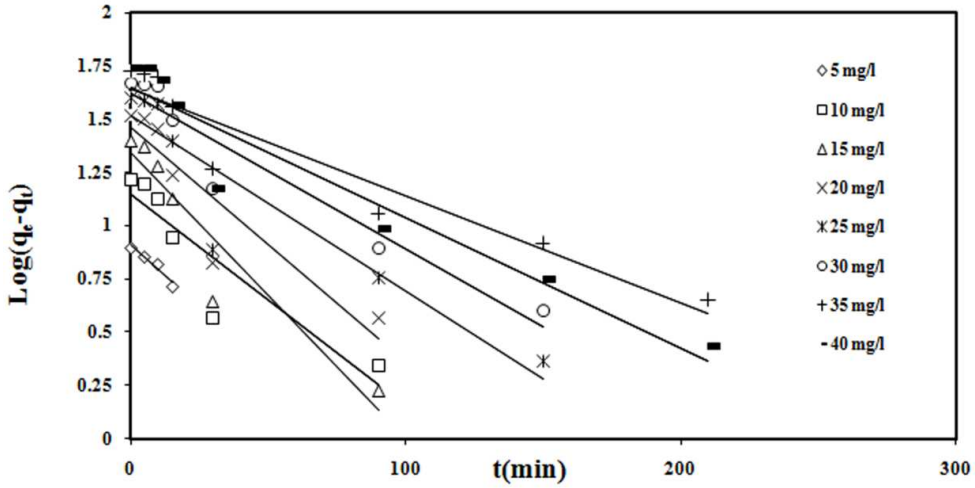

Fig. S.5. *Linear plot of first order model for acid-treated sample over the entire adsorption period.*

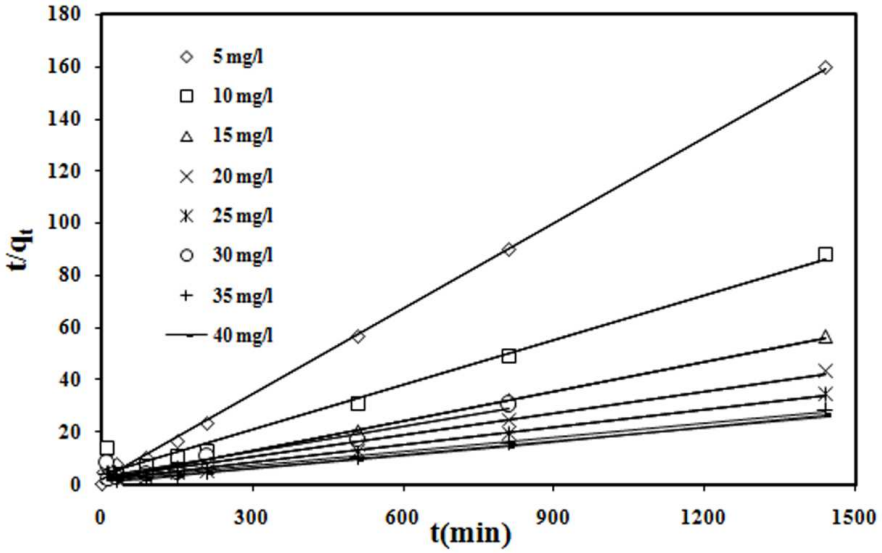

Fig. S.6. *Linear plot of second order model for acid-treated sample over the entire adsorption period.*

Table S.1. *The Bohem titration data for three adsorbents untreated, NaOH treated and H_2SO_4 treated.*

Bohem Titration method					
adsorbent	carboxyl groups	lactone	phenolic	acidity	basictiy
untreated	0.1607	0.0001	0.2443	0.4050	0.0205
treated by NaOH(0.5)	0.2262	0.0785	0.2240	0.5288	0.0068
treated by H_2SO_4(0.01)	0.1548	0.0015	0.1138	0.2700	0.0260

Acknowledgments

The authors would like to gratefully acknowledge Universiti Kebangsaan Malaysia for laboratory and material supports.

List of Symbols

1/n	Constant that related to heterogeneous surface of adsorbent
α_L	Constant related to energy of adsorption (l/mg)
C_o	Concentrations of dye at initial time , t = 0 (mg/l)
C_e	Equilibrium concentration of adsorbate in solution (mg/l)
C_t	Residual Concentration or Concentrations of dye at any time ,t ($mg.L^{-1}$)
k_1	Constant rate for first order (min^{-1})
k_2	Constant rate for second order ($g\ mg^{-1}\ min^{-1}$)
k_f	Constant that related to adsorption capacity
K_L	Constant related to efficiency of solute adsorption (l/g)
m	Mass of adsorbent (g)
q_e	Equilibrium Adsorption Capacity (mg/g)
q_t	Adsorption Capacity at time, t (mg/g)
R_2	Correlation Coefficient
R_L	Dimensionless factor of Langmuir model
t	Time (min)
V	Volume of the solution (L)

References

[1] Belhachemi M., Addoun F., Adsorption of congo red onto activated carbons having different surface properties: studies of kinetics and adsorption equilibrium, Desalination and Water Treatment, 37(2012) 122-129.

[2] Chen S., Zhang J., Zhang C., Yue Q., Li Y., Li C., Equilibrium and kinetic studies of methyl orange and methyl violet adsorption on activated carbon derived from Phragmitesaustries, Desalination, 252 (2010) 149–156.

[3] Mittal A., Malviya A., Kaur D., Mittal J., Kurup L., Studies on the adsorption kinetics and isotherms for the removal and recovery of methyl orange from wastewaters using waste materials, Journal of Hazardous Materials, 148 (2007) 229–240.

[4] Ahmad R., Kumar R., Conducting polyaniline/iron oxide composite: a novel adsorbent for the removal of amido black 10B, Journal of Chemical Engineering Data, 55 (2010) 3489–3493.

[5] K¨orbahti B. K., Rauf M.A., Application of response surface analysis to the photolytic degradation of Basic Red 2 dye., Chemical Engineering Journal, 138 (2008) 166–171.

[6] Atun G., Hisarli G., Tuncay M., Adsorption of safranine-O on hydrophilic and hydrophobic glass surfaces, Colloids and Surfaces A: Physicochemical and Engineering Aspects, 143(1998) 27–33.

[7] Avlonitis S.A., Poulios I., Sotiriou D., Pappas M., Moutesidis K., Simulated cotton dye effluents treatment and reuse by nanofiltration, Desalination, 221 (2008) 259–267.

[8] Han X., Yuan J., Ma X., Adsorption of malachite green from aqueous solutions onto lotus leaf: equilibrium, kinetic, and thermodynamic studies, Desalination and Water Treatment, (2013) 1-12.

[9] Yue Q.Y., Gao B.Y., Wang Y., Zhang H., Sun X., Wang S.G., Gu R.R., Synthesis of polyamine flocculants and their potential use in treating dye wastewater, Journal of Hazardous Materials, 152 (2008) 221–227.

[10] Wang S., A comparative study of Fenton and Fenton-like reaction kinetics in decolourisation of wastewater, Dyes and Pigments, 76 (2008) 714–720.

[11] Hua C., Zhang R., Li L., Zheng X., Adsorption of phenol from aqueous solutions using activated carbon prepared from crofton weed, Desalination and Water Treatment, 37(1-3) (2012) 230-237.

[12] Shih M.-c., Kinetics of the batch adsorption of methylene blue from aqueous solutions onto rice husk: effect of acid-modified process and dye concentration, Desalination and Water Treatment, 37 (1-3) (2012) 200-214.

[13] Ashraf M.A., Rehman M.A, Alias Y., Yusoff I., Removal of Cd(II) onto Raphanus sativus peels biomass: equilibrium, kinetics, and thermodynamics., Desalination and Water Treatment, 51(22-24) (2013) 4402-4412.

[14] Sundrarajan M., Vishnu G., Joseph K., Ozonation of light-shaded exhausted reactive dye bath for reuse, Dyes and Pigments, 75 (2007) 273–278.

[15] Daud N.K., Akpan U.G., Hameed B.H., Decolorization of Sunzol Black DN conc. in aqueous solution by Fenton oxidation process: effect of system parameters and kinetic study, Desalination and Water Treatment, 37(1-3) (2012) 1-7.

[16] Raghu S., Basha C. A., Chemical or electrochemical techniques, followed by ion exchange, for recycle of textile dye wastewater, Journal of Hazardous Materials, 149 (2007) 324–330.

[17] Shih M.Ch., Kinetics of the batch adsorption of methylene blue from aqueous solutions onto rice husk: effect of acid-modified process and dye concentration, Desalination and Water Treatment, 37 (2012) 200-214.

[18] Sulak M.T., Yatmaz H.C., Removal of textile dyes from aqueous solutions with ecofriendly biosorbent, Desalination and Water Treatment, 37(1-3) (2012), 169-177.

[19] Maezawa A., Nakadoi H., Suzuki K., Furusawa T., Suzuki Y. , Uchida S., Treatment of dye wastewater by using photo-catalytic oxidation with sonication, Ultrasonics Sonochemistry, 14 (2007) 615–620.

[20] Rao R.A.K., Khan M.A., Removal, recovery of Cu(II), Cd(II) and Pb(II) ions from single and multimetal systems by batch and column operation on neem oil cake (NOC), Separation and Purification Technology, 57 (2007) 394–402.

[21] Tamai H., Yoshida T., Sasaki M., Yasuda H., Dye adsorption on mesoporous activated carbon fiber obtained from pitch containing yttrium complex, Carbon., 37 (1999) 983–989.

[22] Wu G.-q., Sun X.-y., Hui H., Zhang X., Yan J., Zhang Q.-s., Adsorption of 2,4-dichlorophenol from aqueous solution by activated carbon derived from moso bamboo processing waste. Desalination and Water Treatment, 51 (22-24) (2013) 4603-4612.

[23] Zhuang X., Wan Y., Feng C., Shen Y., Zhao D., Highly efficient adsorption of bulky dye molecules in wastewater on ordered mesoporous carbons, Chemistry of materials, 21 (2009) 706–716.

[24] Abd El-Latifa M.M, Ibrahim A.M., Removal of reactive dye from aqueous solutions by adsorption onto activated carbons prepared from oak sawdust. Desalination and Water Treatment, 20(1-3) (2010) 102-113.

[25] Sharma P., Kaur H., Sharma M., Sahore V., A review on applicability of naturally available adsorbents for the removal of hazardous dyes from aqueous waste, Environmental monitoring and assessment, 183 (2011) 1-45.

[26] Deniz F., Color removal from aqueous solutions of metal-containing dye using pine cone, Desalination and Water Treatment, 51(22-24) (2013) 4573-4581.

[27] Oliveira E.A., Montanher S.F., Rollemberg M.C., Removal of textile dyes by sorption on low-cost sorbents. A case study: sorption of reactive dyes onto Luffa cylindrica. Desalination and Water Treatment, 25(1-3) (2011) 54-64.

[28] Zhu H., Zhang M., Liu Y., Zhang L., Han R., Study of congo red adsorption onto chitosan coated magnetic iron oxide in batch mode, Desalination and Water Treatment, 37 (2012) 46-54.

[29] Soliman E.M., Ahmed S. A., Fadl A.A., Reactivity of sugar cane bagasse as a natural solid phase extractor for selective removal of Fe(III) and heavy-metal ions from natural water samples, Arabian Journal of Chemistry, 4 (2011) 63–70.

[30] Sud D., Mahajan G., Kaur M.P., Agricultural waste material as potential adsorbent for sequestering heavy metal ions from aqueous solutions – A review, Biroresource technology, 99 (2008) 6017–6027.

[31] Xing Y., Liu D., Zhang L.P., Enhanced adsorption of Methylene Blue by EDTAD-modified sugarcane bagasse and photocatalytic regeneration of the adsorbent, Desalination, 259 (2010) 187–191.

[32] Gong R., Jin Y., Jian Chen, Hu Y., Sun J., Removal of basic dyes from aqueous solution by sorption on phosphoric acid modified rice straw, dyes and pigments, 73 (2007) 332-337.

[33] Malekbala M.R., Hosseini S., Yazdi S.K., Masoudi Soltani S., Malekbala M.R., The study of the potential capability of sugar beet pulp on the removal efficiency of two cationic dyes, Chemical Engineering Research and Design, 90(5),(2012) 704-712.

[34] Lataye D.H., Mishra I.M., Mall I.D., Removal of pyridine from aqueous solution by adsorption on bagasse fly ash, Industrial & Engineering Chemistry Research, 45 (2006) 3934–3943.

[35] Goertzen S.L., Theriault K.D., Oickle A.M., Tarasuk A.C., Andreas H.A., Stan-dardization of the Boehm titration. Part I. CO_2 expulsion and endpoint determination, Carbon, 48 (2010) 1252–1261.

[36] Dyke S.F., Floyd A.J., Sainsbury M., Theobald R.S., Organic spectroscopy. An introduction, 2nd edition, Longman, London, 1978.

[37] Zhang J., Lin X., Luo X., Zhang C., Zhu H., A Modified Lignin Adsorbent for the Removal of 2,4,6-Trinitrotoluene, Chemical Engineering Journal, 168 (2011) 1055-1063.

[38] Hosseini S., Khan M.A., Malekbala M.R., Cheah W., Choong T.S.Y., Carbon coated monolith, a mesoporous material for the removal of methyl orange from aqueous phase: Adsorption and desorption studies, Chemical Engineering Journal, 171 (2011) 1124-1131.

[39] Mckay G., El Geundi M., Nassar M.M., Pore diffusion during the adsorption of dyes onto bagasse pith, Process Safe. Environ. Protec., 74 (1996) 277-288.

[40] Sen T.K., Thi M.T., Afroze S., Phan C., Ang M., Removal of anionic surfactant sodium dodecyl sulphate from aqueous solution by adsorption onto pine cone biomass of Pinus Radiate: equilibrium, thermodynamic, kinetics, mechanism and process design., Desalination and Water Treatment, 45(1-3) (2012) 263-275.

[41] Sartape A.S., Mandhare A.M., Salvi P.P, Pawar D.K., Kolekar S.S., Kinetic and equilibrium studies of the adsorption of Cd(II) from aqueous solutions by wood apple shell activated carbon., Desalination and Water Treatment, 51(22-24), (2013), 4638-4650.

[42] Jia Y.F., Thomas K.M., Adsorption of cadmium ions on oxygen surface sites in activated carbon, Langmuir, 16 (2000) 1114–1122.

[43] Barka N., Assabbanea A., Nounahb A., Laanabc L., Aitichou Y., Removal of tex-tile dyes from aqueous solutions by natural phosphate as a new adsorbent, Desalination, 235 (2010) 264–275.

[44] Abou-Mesalam M.M., Sorption kinetics of copper, zinc, cadmium and nickel ions on synthesized silico-antimonate ion exchanger, Colloids and Surfaces A: Physicochemical and Engineering Aspects, 225 (2003) 85–94.

[45] Lagergren S., About the theory of so called adsorption of soluble substances, Kungliga Svenska Vetenskapsakademiens Handlinga, 24 (1898) 1–39.

[46] Ma X., Li L., Yang L., Su C., Wang K., Yuan S., Zhou J., Adsorption of heavy metal ions using hierarchical CaCO3–maltose meso/macroporous hybrid materials: Adsorption isotherms and kinetic studies. Journal of Hazardous Materials, 209–210(0) (2012) 467-477.

[47] Hardani Kh., Buazar F., Ghanemi K., Kashisaz M., Baghlani-Nezhad M. H., Khaledi-Naseb A., Badri M.. Removal of Toxic Mercury (II) from Water via Fe3O4/Hydroxyapatite Nanoadsorbent: An Efficient, Economic and Rapid Approach. AASCIT Journal of Nanoscience. Vol. 1, No. 1, (2015), 11-18.

[48] Elsherbiny A.S., Salem M.A, Ismail A.A., Influence of the alkyl chain length of cyanine dyes on their adsorption by Na+-montmorillonite from aqueous solutions. Chemical Engineering Journal, 200–202(0) (2012) 283-290.

[49] Teoh Y.P., Khan M.A., Choong T.S.Y., Kinetic and isotherm studies for lead adsorption from aqueous phase on carbon coated monolith. Chemical Engineering Journal, 217(0) (2013) 248-255.

[50] Chen B.N., Hui C.W., McKay G., Film-pore diffusion modeling and contact time optimization for the adsorption of dyestuffs on pith, Chemical Engineering Journal, 84 (2001) 77–94.

[51] Valix M., Cheung W.H., McKay G., Preparation of activated carbon using low temperature carbonisation and physical activation of high ash raw bagasse for acid dye adsorption, Chemosphere, 56 (2004) 493–501.

[52] Tsai W.T., Chang C.Y., Lin M.C., Chien S.F., Sun H.F., Hsieh M.F., Adsorption of acid dye onto activated carbons prepared from agricultural waste bagasse by $ZnCl_2$ activation, Chemosphere, 45 (2001), 51–58.

[53] McKay G., El-Geundi M., Nassar M.M., Equilibrium studies for the adsorption of dyes on bagasse pith, Adsorption science & technology, 15 (1997) 251–270.

[54] Juang R.Sh., Wu F.C., Tseng R.L., Characterization and use of activated carbons prepared from bagasses for liquid-phase adsorption, Colloids and Surfaces A: Physicochemical and Engineering Aspects, 201 (2002) 191–199.

[55] Wong S.Y., Tan Y.P., Abdullah A.H., Ong S.T., The removal of basic and reactive dyes using quartenised sugar cane bagasse, Journal of Physical Science, 20 (2009) 59–74.

[56] Ashoka H.S., Inamdar S.S., Adsorption removal of Methyl red from Aqueous solution with treated Sugarcane bagasse and activated carbon- a comparative study, Global Journal of Environmental Research, 4 (2010) 175-182.

[57] Raymundo A.S., Zanarotto R., Belisário M., Pereira M.G., Ribeiro J.N., Ribeiro A.V.F.N., Evaluation of sugar-cane bagasse as bioadsorbent in the textile wastewater treatment contaminated with carcinogenic Congo Red Dye, Brazilian Archives of Biology and Technology, 53 (2010) 931-938.

[58] Ho Y., Chiu W., Wang C., Regression analysis for the sorption isotherms of basic dyes on sugarcane dust, Bioresource Technology, 96(2005a) 1285–1291.

[59] Filho N.C., Venancio E.C., Barriquello M.F., Hechenleitner A.A., Pineda E.A.G., Methylene blue adsorption onto modified lignin from sugarcane baggasse, Eclectic Chemistry, 32(2007) 63–70.

[60] Azhar S.S., Liew A.G., Suhardy D., Hafiz K.F., Hatim M.D.I., Dye removal from aqueous solution byusing adsorption on treated sugarcane baggase, American Journal of Applied Sciences. 2(2005) 1499– 1503.